

## “Explosive” Synthesis of Metal-Formate Frameworks for Methane Capture: An Experimental and Computational Study

Received 00th January 20xx,  
Accepted 00th January 20xx

Xiao-Wei Liu,<sup>a,b,c</sup> Ya Guo,<sup>a,c</sup> Andi Tao,<sup>b</sup> Michael Fischer,<sup>d,e</sup> Tian-Jun Sun,<sup>a\*</sup> Peyman Z. Moghadam,<sup>b\*</sup> David Fairen-Jimenez<sup>b\*</sup> and Shu-Dong Wang<sup>a,f\*</sup>

DOI: 10.1039/x0xx00000x

www.rsc.org/

**In this work, we show a solvent-free “explosive” synthesis (SFES) method for the ultrafast and low-cost synthesis of metal-formate frameworks (MFFs). A combination of experiments and in-depth molecular modelling analysis – using grand canonical Monte Carlo (GCMC) simulations – of the adsorption performance of the synthesized nickel formate framework (Ni-FA) revealed extremely high quality products with permanent porosity, prominent CH<sub>4</sub>/N<sub>2</sub> selectivity (ca. 6.0), and good CH<sub>4</sub> adsorption capacity (ca. 0.80 mmol g<sup>-1</sup> or 33.97 cm<sup>3</sup> cm<sup>-3</sup>) at 1 bar and 298 K. This performance is superior to that of many other state-of-the-art porous materials.**

**Natural gas (NG), mainly composed of methane, is a clean and cheap alternative to more contaminative fossil fuels such as oil and coal.<sup>1</sup> The free emissions of methane, however, are also regarded as the most important non-CO<sub>2</sub> greenhouse gas contributing to global warming.<sup>2</sup> Indeed, large sources of NG, with methane concentrations in the range of 5–75% (medium) or <5% (dilute) purity,<sup>3</sup> are unfortunately often simply flared in small or inconvenient flows.<sup>4</sup> In this sense, concentrating dilute methane sources to medium purity for combustion applications, or upgrading medium quality streams to high purity (>90%) to meet pipeline quality, is extremely desirable to effectively utilize the energy and make direct gas or liquid end-products.<sup>3</sup> Among all other NG components, nitrogen has very similar physical properties to methane (Table S3),<sup>5</sup> and therefore their separation is extremely difficult, becoming a critical**

issue to make the most of NG resources.<sup>6</sup> Currently, cryogenic distillation is employed for CH<sub>4</sub>/N<sub>2</sub> separation, but is highly energy intensive and inflexible, especially for small-scale plants.<sup>1</sup> In the cases of dilute flows with low methane concentration, the capture of methane, rather than nitrogen, is probably a wiser choice for the sake of saving costs, in which both the selectivity and adsorption capacity matter.

A myriad of adsorption-based strategies have been developed for CH<sub>4</sub>/N<sub>2</sub> separation. Nevertheless, the proposed adsorbents suffer from high costs, low selectivities and/or capacities.<sup>7</sup> Metal-formate frameworks (MFFs),<sup>8</sup> a subclass of the metal-organic frameworks (MOFs) family,<sup>9</sup> have been reported to exhibit higher CH<sub>4</sub>/N<sub>2</sub> selectivities than other porous materials.<sup>10</sup> MFFs are arguably the simplest MOFs that can be synthesized. Their short and low toxic formate ligands make them cheap and environment-friendly materials.<sup>8</sup> As an example of an MFF, Figure 1 shows the structure of the nickel formate framework (Ni-FA) and the one-dimensional zigzag channels of 4–6 Å emerging from the different orientations of the formate groups.

Porous MFFs have been synthesized via three main different routes: i) recrystallization of metal(II) formate dehydrates,<sup>11</sup> ii) solution chemistry,<sup>12</sup> and iii) conventional solvothermal reactions.<sup>13</sup> However, these methods still present some challenges. First, recrystallization sometimes needs to be operated at high temperature, e.g. 170 °C for 40 h, a much higher temperature than the boiling point of formic acid.<sup>11</sup> Second, the solution-diffusion strategy usually requires

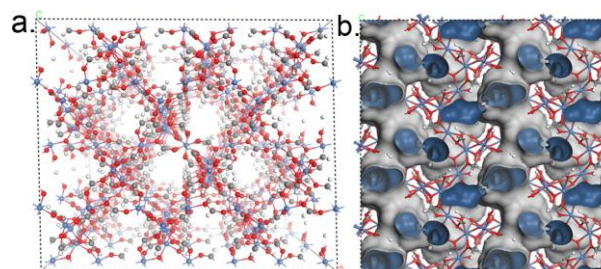


**Figure 1.** Schematics showing **a.** the structure of Ni-FA looking through y-axis and **b.** the one-dimensional zigzag pores looking through x-axis. Framework atoms: Ni (cyan), C (gray), O (red) and H (white).

<sup>a</sup> Dalian National Laboratory for Clean Energy, Dalian Institute of Chemical Physics, Chinese Academy of Sciences, 457 Zhongshan Road, Dalian 116023, P. R. China. Email: wangsd@dicp.ac.cn; suntianjun@dicp.ac.cn

<sup>b</sup> Department of Chemical Engineering & Biotechnology, University of Cambridge, Philippa Fawcett Drive, Cambridge CB3 0AS, United Kingdom, Email: df334@cam.ac.uk; pzm20@cam.ac.uk

<sup>c</sup> University of Chinese Academy of Sciences, 19A Yuquan Road, Beijing 100049, P. R. China

<sup>d</sup> Crystallography group, Department of Geosciences, University of Bremen, Klagenfurter Straße 2-4, D-28359 Bremen, Germany

<sup>e</sup> MAPEX Center for Materials and Processes, University of Bremen, D-28359 Bremen, Germany

<sup>f</sup> State Key Laboratory of Catalysis, Dalian Institute of Chemical Physics, Chinese Academy of Sciences, 457 Zhongshan Road, Dalian 116023, P. R. China

† Electronic Supplementary Information (ESI) available: [Experiment, characterization and simulation details etc.]. See DOI: 10.1039/x0xx00000x

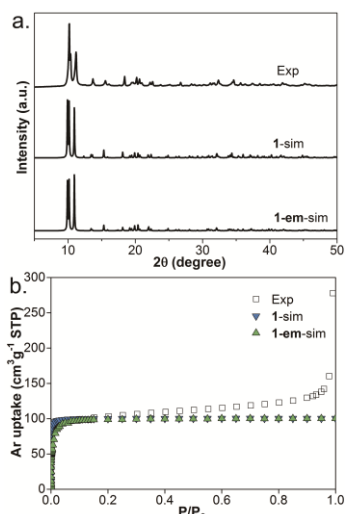


**Figure 2.** a. PXRD patterns of the experimental Ni-FA-SFES, 1-simulated and 1-em-simulated samples. b. Argon adsorption isotherms of experimental Ni-FA-SFES (black empty squares), and simulated samples: 1-simulated (blue inverted triangles); 1-em-simulated (green triangles) at 87 K.

bulky templates.<sup>12</sup> Third, the solvothermal route demands large amounts of organic solvents.<sup>13b, 14</sup> Besides, the first two methods also found difficulties when synthesizing some MFFs, such as Ni-FA.<sup>11a, 12b</sup>

Redox reactions take place everywhere in life; they are widespread in the production of important industrial chemicals such as sulfuric acid and ammonia.<sup>15</sup> Looking for a new synthesis approach and inspired by the high reductibility of formic acid, we attempted to employ metallic nitrates – which own high oxidizability because of the nitrate radicals – to initiate a redox process for synthesizing MFFs, specifically for Ni-FA ( $[\text{Ni}_3(\text{HCOO})_6]$ ). We called this method “solvent-free explosive synthesis”, i.e. SFES. Using this method, we found the process is extremely fast and, more interestingly, it does not require organic solvents or templates. To the best of our knowledge, this is the first case that a MFF, or a MOF, can be rapidly produced in such a simple way. In addition, we used the grand canonical Monte Carlo (GCMC) simulations, which are very useful techniques in MOF screening and mechanism investigation in adsorption and separation of gas molecules,<sup>16</sup> to complement the study of the adsorption performance of the Ni-FA synthesized, which showed an excellent agreement with experiments. Combining our experimental and computational approach, we demonstrated that Ni-FA revealed extremely high quality products, high selectivities and adsorption capacities for capturing methane from  $\text{CH}_4/\text{N}_2$  mixtures, which is in particular promising to deal with lean methane sources.

We conducted the SFES route to produce Ni-FA by directly mixing nickel nitrate hexahydrate and formic acid at different ratios at room temperature. A video included in the ESI shows the advance of a typical reaction, which started slowly, then evolved into a fierce reaction in ca. two minutes, and finally finished after six minutes. During the process, nitrogen dioxide – a brownish gas – was released from the reaction, indicating a strong evidence for the presence of redox reactions (see the supplementary video). Scheme S1 gives a possible mechanism for the redox reactions. After washing the resulting green

solids in acetone and drying them under vacuum, we collected their powder X-ray diffraction (PXRD) patterns. Interestingly, we found that it was possible to utilize a wide range of metal/acid ratios, from ca. 1:4 to 1:15 (Figure S1), to produce successfully the desired Ni-FA product, revealing a remarkable synthesis flexibility compared to other traditional methods mentioned above. At this point, we selected the 1:7 ratio since it has been widely used in solvothermal synthesis before,<sup>10a, 17</sup> and also returned a good product crystallinity in our work. Figure 2a reveals that the intense peaks in the product profile match well those present in the simulated structure of Ni-FA.<sup>11a</sup> To test the stability of the products, we extended our PXRD analysis to higher temperatures. Figure S2 shows that Ni-FA-SFES (the Ni-FA sample prepared using the SFES method) maintained its structure up to 250 °C, and no phase transition or intensity change in the peaks were observed before the framework decomposition at 300 °C. Figure S3 gives the thermo-gravimetric analysis (TGA) profile of Ni-FA-SFES, which proves the framework was indeed thermally stable up to 270 °C, similar to previously reported Ni-FA<sup>18</sup> and its Co and Fe analogues.<sup>12b, 14</sup>

Figure 2b shows the excellent agreement between experimental and GCMC simulated argon adsorption isotherms at 87 K on the structure 1 of Ni-FA. Structure 1 was obtained from the as-synthesized structure by optimising the reported structural parameters using DFT calculations (see details in the ESI).<sup>11a</sup> Since GCMC simulations are run on a perfect crystal, the excellent agreement indicates a high quality of the experimental Ni-FA synthesized. The experimental pore size distribution (PSD), using a standard NLDFT model, and the geometrical one obtained through simulations on 1 are both centred at ca. 5 Å (Figure S4). Further to Ar isotherms, Figure S5 shows the experimental and simulated pure  $\text{CH}_4$  and  $\text{N}_2$  adsorption isotherms at 298 K. Interestingly, the simulations on structure

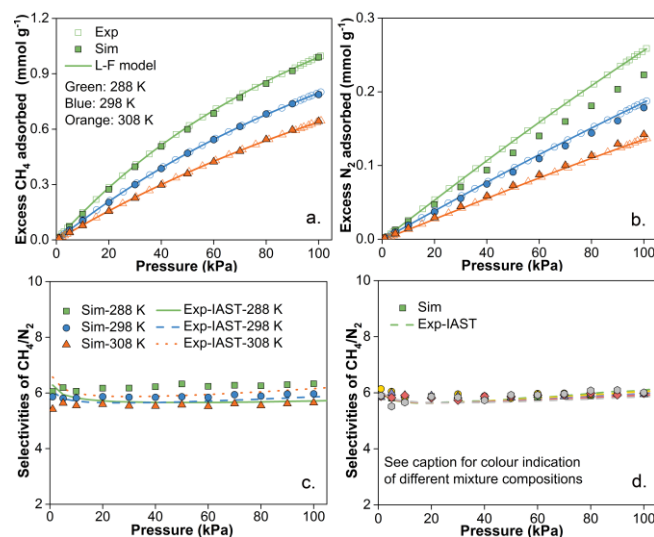


**Figure 3** a. Pure  $\text{CH}_4$  and b.  $\text{N}_2$  adsorption isotherms of experimental Ni-FA-SFES (empty symbols), GCMC simulated 1-em (filled symbols). Lines indicate Langmuir-Freundlich (L-F) model fitting on experimental isotherms;<sup>19</sup> IAST selectivities of Ni-FA-SFES and GCMC 1-em-simulated selectivities for c. equimolar mixtures at different temperatures and d. different mixture compositions:  $\text{CH}_4$ :  $\text{N}_2$ , 0.5:0.5 (green), 0.6:0.4 (yellow), 0.7:0.3 (purple), 0.8:0.2 (red) and 0.9:0.1 (grey) at 298 K.

**1** under-predict the amount adsorbed. We then decided to run a new simulation on a geometrically energy minimised (**em**) structure that allows reallocating the atoms of the MOF but keeping the same cell parameters; we called this structure **1-em**. The new simulated isotherms are able to match the experimental curves. When comparing the two structures, the helium void fraction and helium accessible volume increased slightly from 0.229 to 0.278, and 0.121 to 0.147 cm<sup>3</sup> g<sup>-1</sup> for **1** and **1-em**, respectively. The change of the structure is also reflected in the PSD, where the size incremented slightly for **1-em** (Figure S4). An overlay of both **1** and **1-em** structures shows minor reorientations of the formate linkers (Figure S6), something that has been observed previously on other MOFs such as ZIF-8.<sup>20</sup> Figures 3a-b show the excellent agreement between experimental and simulated pure gas adsorption isotherms at different temperatures, further confirming the importance of small structural changes in **1-em**.

In order to evaluate the separation performance of Ni-FA for CH<sub>4</sub>/N<sub>2</sub> mixtures, we calculated the selectivity based on Henry's law and Ideal Adsorbed Solution Theory (IAST) from pure component experimental isotherms. To evaluate the goodness of such approach, we compared these selectivities with those obtained through GCMC simulations: we obtained simulated Henry's law selectivity based on the Widom insertion method,<sup>21</sup> whereas equilibrium selectivity was directly obtained from GCMC binary gas simulations. Table S5 lists the selectivities obtained from Henry's law, in the range of 5.4~7.0 at different temperatures, showing excellent agreement between experiments and simulations. These results are also comparable to those of the previously reported Ni-FA sample prepared using conventional solvothermal methods (Ni-FA-SS).<sup>10a</sup> Figures 3c-d show the comparison of IAST and binary mixtures GCMC results at different temperatures and compositions, respectively. The selectivities for equimolar mixtures present similar values over the pressure range at different temperatures, while the consistently high selectivity is independent of the gas compositions in e.g. medium or dilute sources. All these also confirm the validity of the IAST approach to predict selectivities from pure component experimental isotherms.

Figure 4a compares the CH<sub>4</sub>/N<sub>2</sub> selectivities of well-known adsorbents, in which most of the selectivity values are below 5 while Ni-FA shows a prominent value of ca. 6. In addition, Ni-FA-SFES also shows a good adsorption capacity (ca. 0.80 mmol g<sup>-1</sup>, or a high volumetric capacity of 33.97 cm<sup>3</sup> cm<sup>-3</sup> based on the framework density) at 1 bar and 298 K and a low cost free-solvent synthesis, which make it a promising candidate for methane capture from CH<sub>4</sub>/N<sub>2</sub> mixtures. Since the typical composition of coal-mine ventilation air - a large-scale dilute methane source of high-impact is ca. 1% CH<sub>4</sub>, 1% CO<sub>2</sub> and 98% N<sub>2</sub> at atmospheric pressure, we simulated this composition on Ni-FA. Figure S7 shows the adsorption isotherms and selectivities. Ni-FA has a consistent CH<sub>4</sub>/N<sub>2</sub> selectivity of ca. 6.0 and a relatively but still interesting CH<sub>4</sub> adsorption capacity of ca. 0.01 mmol g<sup>-1</sup>. In applications such as combustion, a high selectivity > 5 is essentially required to create an output stream > 5% CH<sub>4</sub> (the flammability limit in air) from a starting CH<sub>4</sub> con-

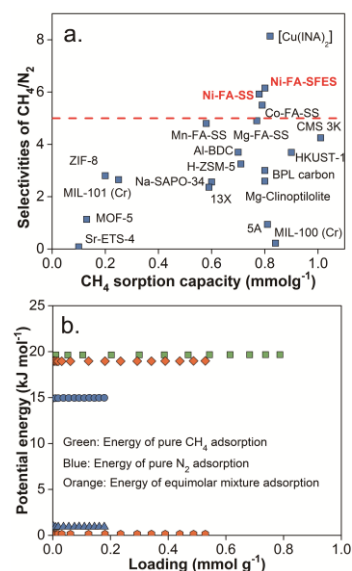


**Figure 4.** a. Selectivities of CH<sub>4</sub>/N<sub>2</sub> and the CH<sub>4</sub> sorption capacity of some of state-of-the-art adsorbents at 1 bar and 298 K (see details in Table S7). The Ni-FA-SS selectivity value is reported for the sample synthesized using the same reagents as the SFES method in DMF; b. Host-adsorbate potential energy breakdown at 298 K. Square: vdW energy of pure CH<sub>4</sub> adsorption; circle (triangle): vdW (Coulombic) energy of pure N<sub>2</sub> adsorption; diamond (hexagon): vdW (Coulombic) energy of equimolar mixture adsorption. Adsorbate-adsorbate interactions are too small and removed for clarity.

centration of ca. 1% in one cycle.<sup>3</sup> On the other hand, the CO<sub>2</sub>/CH<sub>4</sub> selectivity is, as expected, remarkably high, leading to high amount of CO<sub>2</sub> in the adsorbed phase. An optimal solution would be integrating a previous step to remove CO<sub>2</sub> before capturing CH<sub>4</sub>, as removing CO<sub>2</sub> from N<sub>2</sub> is generally easier to achieve.<sup>22</sup> We then applied a new simulation without CO<sub>2</sub> and new CH<sub>4</sub> and N<sub>2</sub> concentrations (1% and 99%). Results prove the high selectivity was maintained in this case, resulting in a desirable concentration of CH<sub>4</sub> (5.5 %) in the adsorbed phase at 1 bar (Figure S8).

In order to look deeper into the separation process and the high CH<sub>4</sub>/N<sub>2</sub> selectivity found for Ni-FA, we studied the density distributions of the adsorbed gas molecules. Figures S9-S12 show those profiles obtained from the simulations of equimolar mixture adsorption at 298 K and different pressures. From infinite dilution region to 1 bar, the profiles clearly show methane and nitrogen molecules were only favorably adsorbed at two localized adsorption sites with similar surrounding environment. This phenomenon maybe mainly due to the reduced freedom of movement of the molecules in the limited cavities, which was also found in the adsorption of H<sub>2</sub> on Mg-FA at high pressures.<sup>23</sup> Owing to different orientations of the formate ligands, these areas are actually the kinks of the zigzag channels with one HCOO<sup>-</sup> group pointing inwards (Figure S13), and therefore accompanied by a large density of framework atoms providing high overlap potentials derived from van der Waals (vdW) interactions. DFT calculations in previous work also delivered very similar favourite adsorption sites for the adsorption of CH<sub>4</sub> and N<sub>2</sub> on Mg-FA.<sup>10b</sup> As a consequence, the competition of gas molecules for these preferential sites will dictate the final selectivity. Figure 4b shows the potential energy breakdown for the vdW and Coulombic interactions: adsorbate-adsorbate interactions

are pretty small for both pure gases and mixtures over the pressure range. Coulombic interactions only account for ca. 6% of the overall potential energy in the adsorption of pure N<sub>2</sub> and less than 1% in the adsorption of mixtures. In sharp contrast, host-adsorbate vdW interactions dominate the overall potential energy, both for the pure gases and mixtures. In particular, CH<sub>4</sub> show stronger vdW interactions with Ni-FA than N<sub>2</sub> (ca. 20 kJ mol<sup>-1</sup> vs. 15 kJ mol<sup>-1</sup>), in line with the energy difference (ca. 5 kJ mol<sup>-1</sup>) calculated from DFT simulations for individual adsorption sites of the two adsorbates on different MFFs.<sup>10b</sup> All in all, this distinct difference gives rise to the higher isosteric heat of adsorption (Q<sub>st</sub>) of CH<sub>4</sub> than N<sub>2</sub> (Figure S14), and the prominent CH<sub>4</sub>/N<sub>2</sub> selectivity in the end.

In this work, we show how a porous MFF, Ni-FA, is rapidly synthesized using a solvent-free “explosive” synthesis (SFES) method that does not involve the use of organic solvents or templates. The resulting nickel-formate framework is cheap and thermally stable. It also has high product quality and superior CH<sub>4</sub>/N<sub>2</sub> separation performance to most of other porous materials. We also used GCMC simulations to investigate deeply the adsorption and separation performance of Ni-FA for CH<sub>4</sub>/N<sub>2</sub> mixtures. We showed that the higher vdW interactions of CH<sub>4</sub> molecules with the large density of framework atoms at the channel kinks gave rise to the high selectivity of CH<sub>4</sub>/N<sub>2</sub> of Ni-FA. Ultimately, Ni-FA shows great potential for the capture of methane from nitrogen in mixtures for real-world applications.

Our study shed light on producing MOFs containing potential oxidising and reducing units via redox reactions. Although we recently found metal acetates and formic acid could also be utilized to initiate a metathetically solvent-free reaction for the synthesis of MFFs,<sup>24</sup> the SFES method, driven by the redox reactions, is much faster than the former. We believe this SFES method has further potential for the synthesis of other compounds, such as the formate-based perovskite structures,<sup>25</sup> or other cases when properties like magnetism are of interest.<sup>26</sup>

## Notes and references

- ‡ X.-W. L. greatly appreciates the support from China Scholarship Council (CSC) and British Council (Newton fund). T.-J. S. and S.-D. W. are grateful to NSFC China for funding (Grant No. 21776266 and 21476231). D. F.-J. thanks the Royal Society for funding through a University Research Fellowship. M. F. gratefully acknowledges funding by the Central Research Development Fund (CRDF) of the University of Bremen (Funding line 04-Independent Projects for Post-Docs). Computational work was supported by the Cambridge High Performance Computing Cluster, Darwin.
- J. W. Yoon, H. Chang, S.-J. Lee, Y. K. Hwang, D.-Y. Hong, S.-K. Lee, J. S. Lee, S. Jang, T.-U. Yoon, K. Kwac, Y. Jung, R. S. Pillai, F. Faucher, A. Vimont, M. Daturi, G. Férey, C. Serre, G. Maurin, Y.-S. Bae and J.-S. Chang, *Nat. Mater.*, 2017, **16**, 526-531.
  - E. S. Kadantsev, P. G. Boyd, T. D. Daff and T. K. Woo, *J. Phys. Chem. Lett.*, 2013, **4**, 3056-3061.
  - J. Kim, A. Maiti, L.-C. Lin, J. K. Stolaroff, B. Smit and R. D. Aines, *Nat. Commun.*, 2013, **4**, 1694.
  - D. A. Kennedy, M. Mujcin, E. Trudeau and F. H. Tezel, *J. Chem. Eng. Data*, 2016, **61**, 3163-3176.
  - K. Lee, W. C. Isley, A. L. Dzubak, P. Verma, S. J. Stoneburner, L. C. Lin, J. D. Howe, E. D. Bloch, D. A. Reed, M. R. Hudson, C. M. Brown, J. R. Long, J. B. Neaton, B. Smit, C. J. Cramer, D. G. Truhlar and L. Gagliardi, *J. Am. Chem. Soc.*, 2014, **136**, 698-704.
  - M. Tagliabue, D. Farrusseng, S. Valencia, S. Aguado, U. Ravon, C. Rizzo, A. Corma and C. Mirodatos, *Chem. Eng. J.*, 2009, **155**, 553-566.
  - a) R. T. Yang, *Adsorbent: Fundamentals and Applications*, John Wiley & Sons, Hoboken, 2003; b) X.-W. Liu, J.-L. Hu, T.-J. Sun, Y. Guo, T. D. Bennett, X.-Y. Ren and S.-D. Wang, *Chem. Asian J.*, 2016, **11**, 3014-3017.
  - R. Shang, S. Chen, Z.-M. Wang and S. Gao, in *Encyclopedia of Inorganic and Bioinorganic Chemistry*, John Wiley & Sons, Ltd, 2011.
  - P. Z. Moghadam, A. Li, S. B. Wiggin, A. Tao, A. G. P. Maloney, P. A. Wood, S. C. Ward and D. Fairen-Jimenez, *Chem. Mater.*, 2017, **29**, 2618-2625.
  - a) X. Ren, T. Sun, J. Hu and S. Wang, *RSC Adv.*, 2014, **4**, 42326-42336; b) M. Fischer, *Micropor. Mesopor. Mater.*, 2016, **219**, 249-257.
  - a) M. Viertelhaus, P. Adler, R. Clérac, Christopher E. Anson and Annie K. Powell, *Eur. J. Inorg. Chem.*, 2005, **2005**, 692-703; b) M. Viertelhaus, C. E. Anson and A. K. Powell, *Z. Anorg. Allg. Chem.*, 2005, **631**, 2365-2370.
  - a) Z. Wang, B. Zhang, H. Fujiwara, H. Kobayashi and M. Kurmoo, *Chem. Commun.*, 2004, 416-417; b) Z. Wang, B. Zhang, M. Kurmoo, M. A. Green, H. Fujiwara, T. Otsuka and H. Kobayashi, *Inorg. Chem.*, 2005, **44**, 1230-1237.
  - a) J. A. Rood, B. C. Noll and K. W. Henderson, *Inorg. Chem.*, 2006, **45**, 5521-5528; b) D. N. Dybtsev, H. Chun, S. H. Yoon, D. Kim and K. Kim, *J. Am. Chem. Soc.*, 2003, **126**, 32-33.
  - Z. M. Wang, Y. J. Zhang, T. Liu, M. Kurmoo and S. Gao, *Adv. Funct. Mater.*, 2007, **17**, 1523-1536.
  - E. Kostiner and N. Jespersen, in *Chemistry (Barron's EZ-101 Study Keys)*, 2nd ed, Barron's Educational Series, 2003.
  - a) Z. Qiao, C. Peng, J. Zhou and J. Jiang, *J. Mater. Chem.*, 2016, **4**, 15904-15912; b) Z. Qiao, N. Wang, J. Jiang and J. Zhou, *Chem. Commun.*, 2016, **52**, 974-977.
  - K. H. Li, D. H. Olsan, J. Y. Lee, W. H. Bi, K. Wu, T. Yuen, Q. Xu and J. Li, *Adv. Funct. Mater.*, 2008, **18**, 2205-2214.
  - Z. M. Wang, B. Zhang, Y. J. Zhang, M. Kurmoo, T. Liu, S. Gao and H. Kobayashi, *Polyhedron*, 2007, **26**, 2207-2215.
  - R. Sips, *J. Chem. Phys.*, 1948, **16**, 490-495.
  - D. Fairen-Jimenez, S. A. Moggach, M. T. Wharmby, P. A. Wright, S. Parsons and T. Düren, *J. Am. Chem. Soc.*, 2011, **133**, 8900-8902.
  - B. Widom, *J. Chem. Phys.*, 1963, **39**, 2808-2812.
  - K. Sumida, D. L. Rogow, J. A. Mason, T. M. McDonald, E. D. Bloch, Z. R. Herm, T.-H. Bae and J. R. Long, *Chem. Rev.*, 2012, **112**, 724-781.
  - A. Rossin, D. Fairen-Jimenez, T. Düren, G. Giambastiani, M. Peruzzini and J. G. Vitillo, *Langmuir*, 2011, **27**, 10124-10131.
  - Unpublished results.
  - G. P. Nagabhushana, R. Shivaramaiah and A. Navrotsky, *J. Am. Chem. Soc.*, 2015, **137**, 10351-10356.
  - P. Dechambenoit and J. R. Long, *Chem. Soc. Rev.*, 2011, **40**, 3249-3265.